Anal. Chem. **2004,** *76,* 2406−2410

Quantum Dot-Encoded Mesoporous Beads with High Brightness and Uniformity: Rapid Readout Using Flow Cytometry

Xiaohu Gao and Shuming Nie*

Wallace H. Coulter Department of Biomedical Engineering, Emory University and Georgia Institute of Technology, 1639 Pierce Drive, Suite 2001, Atlanta, Georgia 30322 and Departments of Chemistry, Hematology, Oncology, and the Winship Cancer Institute, Emory University, 1365 Clifton Road, Suite B4100, Atlanta, Georgia 30322

A new generation of optically encoded beads has been prepared by using mesoporous polystyrene beads and surfactant-coated semiconductor quantum dots. In comparison with nonporous beads of similar sizes and chemical compositions, the encoded porous beads are ∼1000 times brighter and 5 times more uniform in fluorescence intensities. Using both absolute intensity and ratiometric fluorescence coding, we show that the beads can be identified with a standard flow cytometer at 1000 beads/s. This result indicates that the multiple excited-state lifetimes and relaxation pathways of quantum dots do not limit their applications in high-speed optical detection and imaging.

Micrometer-sized particles with embedded spectroscopic signatures are of considerable interest in analytical chemistry and bioengineering due to their potential applications in multiplexed bioassays, medical diagnostics, drug screening, and combinatorial chemical synthesis.[1−4] Recent advances in several groups have led to a burst of activities on optical "bar coding" based on the use of segmented nanorods,[5,6] porous silicon,[7] rare-earth doped glass,[8] fluorescent silica colloids,[9,10] photobleached patterns,[11] oligonucleotide-linked colloidal gold,[12,13] enhanced Raman nanoparticles,[14,15] and semiconductor quantum dots (QDs).[16−20] While each of these technologies has its advantages and limitations, research in our group has shown that luminescent QDs are ideal fluorophores for optical bar coding because their fluorescence emission wavelengths can be tuned continuously by changing the particle size, and a single wavelength can be used for simultaneous excitation of different-sized QDs.[16−18] High-quality CdSe, CdTe, and alloyed QDs are also stable against photobleaching and have narrow and symmetrical emission peaks.[21−25] In principle, multiple QD colors and intensities can be used to encode thousands or even millions of genes, proteins, and small-molecule compounds.[16] However, the current brightness and uniformity of bar coding signals do not allow bead identification at high speeds and high accuracies. Recent work[17] has used mesoporous silica beads (with nanometer-scale pores) to improve the coding signal brightness, but the silica beads were not sufficiently uniform in size and internal structure, and their fluorescence intensities were found to vary from bead to bead by nearly 50%.

In this paper, we report a new generation of QD-encoded beads based on mesoporous polystyrene beads and surfactant-coated (hydrophobic) QDs. Prepared by a multiple-stage polymerization process, this class of porous beads is highly uniform in size (15.4 ± 0.2 μm diameter) and contains an extensive network of nanometer-sized pores. These "mesoscopic" pores allow rapid

* Corresponding author. Tel: 404-712-8595. E-mail: snie@emory.edu.

(1) Penn, S. G.; He, L.; Natan, M. J. *Curr. Opin. Chem. Biol.* **2003**, *7*, 609−615.
(2) Braeckmans, K.; De Smedt, S. C.; Leblans, M.; Pauwels, R.; Demeester, J. *Nat. Rev. Drug Discovery* **2002**, *1*, 447−456.
(3) Meza, M. B. *Drug Discovery Today* **2000**, *1* (HTS Suppl.), 38−41.
(4) Walt, D. R. *Curr. Opin. Chem. Biol.* **2002**, *6*, 689−695.
(5) Nicewarner-Pena, S. R.; Freeman, R. G.; Reiss, B. D.; He, L.; Pena, D. J.; Walton, I. D.; Cromer, R.; Keating, C. D.; Natan, M. J. *Science* **2001**, *294*, 137−141.
(6) Walton, I. D.; Norton, S. M.; Balasingham, A.; He, L.; Oviso, D. F., Jr.; Gupta, D.; Raju, P. A.; Natan, M. J.; Freeman, R. G. *Anal. Chem.* **2002**, *74*, 2240−2247.
(7) Cunin, F.; Schmedake, T. A.; Link, J. R.; Li, Y. Y.; Koh, J.; Bhatia, S. N.; Sailor, M. J. *Nat. Mater.* **2002**, *1*, 39−41.
(8) Dejneka, M. J.; Streltsov, A.; Pal, S.; Frutos, A. G.; Powell, C. L.; Yost, K.; Yuen, P. K.; Muller, U.; Lahiri, J. *Proc. Natl. Acad. Sci. U.S.A.* **2003**, *100*, 389−393.
(9) Grondahl, L.; Battersby, B. J.; Bryant, D.; Trau, M. *Langmuir* **2000**, *16*, 9709−9715.
(10) Battersby, B. J.; Bryant, D.; Meutermans, W.; Matthews, D.; Smythe, M. L.; Trau, M. *J. Am. Chem. Soc.* **2000**, *122*, 2138−2139.
(11) Braeckmans, K.; de Smedt, S.; Roelant, C.; Leblans, M.; Pauwels, R.; Demeester, J. *Nat. Mater.* **2003**, *2*, 169−193.
(12) Cao, Y. C.; Jin, R.; Nam, J. M.; Thaxton, C. S.; Mirkin, C. A. *J. Am. Chem. Soc.* **2003**, *125*, 14676−14677.
(13) Cao, Y. C.; Jin, R.; Mirkin, C. A. *Science* **2002**, *297*, 1536−1540.
(14) Mulvaney, S. P.; Musick, M. D.; Keating, C. D.; Natan, M. J. *Langmuir* **2003**, *19*, 4784−4790.
(15) Doering, W. E.; Nie, S. *Anal. Chem.* **2003**, *75*, 6171−6176.
(16) Han, M. Y.; Gao, X. H.; Su, J. Z.; Nie, S. M. *Nat. Biotechnol.* **2001**, *19*, 631−635.
(17) Gao, X. H.; Nie, S. M. *J. Phys. Chem. B* **2003**, *107*, 11575−11578.
(18) Gao, X. H.; Chan, W. C. W.; Nie, S. M. *J. Biomed. Opt.* **2002**, *7*, 532−537.
(19) Gaponik, N.; Radtchenko, I. L.; Sukhorukov, G. B.; Weller, H.; Rogach, A. L. *Avd. Mater.* **2002**, *14*, 879−882.
(20) Xu, H.; Sha, M. Y.; Wong, E. Y.; Uphoff, J.; Xu, Y.; Treadway, J. A.; Truong, A.; O'Brien, E.; squith, S.; Stubbins, M.; Spurr, N. K.; Lai, E. H.; Mahoney, W. *Nucleic Acids Res.* **2003**, *31*, e43.
(21) Dabbousi, B. O.; Rodriguez-Viejo, J.; Mikulec, F. V.; Heine, J. R.; Mattoussi, H.; Ober, R.; Jensen, K. F.; Bawendi, M. G. *J. Phys. Chem. B* **1997**, *101*, 9463−9475.
(22) Peng, Z. A.; Peng, X. G. *J. Am. Chem. Soc.* **2001**, *123*, 183−184. Qu, L.; Peng, Z. A.; Peng, X. *Nano Lett.* **2001**, *1*, 333−337.
(23) Zhong, X.; Feng, Y.; Knoll, W.; Han, M. *J. Am. Chem. Soc.* **2003**, *125*, 13559−13563.
(24) Zhong, X.; Han, M.; Dong, Z.; White, T. J.; Knoll, W. *J. Am. Chem. Soc.* **2003**, *125*, 8589−8594.
(25) Bailey, R. E.; Nie, S. *J. Am. Chem. Soc.* **2003**, *125*, 7100−7106.

10.1021/ac0354600 CCC: $27.50
Published on Web 03/13/2004

uptake and immobilization of quantum dots through strong hydrophobic interactions between the pore walls and the QD capping ligands (tri-*n*-octylphosphine oxide, TOPO). As a result, the doped beads are more than 1000 times brighter and 5 times more uniform in fluorescence intensities than nonporous beads of the same size. We show that the encoded porous beads can be identified by using a standard flow cytometer at a readout speed as high as 1000 beads/s. This result indicates that the relatively long excited-state lifetimes (20−50 ns) of quantum dots do not limit their applications in high-speed detection and imaging.

EXPERIMENTAL SECTION

Materials. Core−shell quantum dots (ZnS-capped CdSe) were synthesized according to literature procedures.[21,22] The resulting quantum dots were coated with a layer of TOPO, which was used as a high-temperature coordinating solvent. The QD's fluorescence quantum yields were 20−50% at room temperature, with size variations of 5−10%. Polystyrene microspheres (15.4 ± 0.2 μm diameter) were obtained from Bangs Laboratories (Fishers, IN). Mesoscale pores were generated by extraction of "porogens" such as linear soluble polymers and methyl methacrylate from the beads after synthesis.[26−29] Previous research showed that the pore sizes were in the 2−50-nm range (pore diameter).[27,28] This mixture of small and large pores was favorable for doping because the larger pores would allow rapid QD diffusion and the smaller pores would provide more surface area for stable QD immobilization. In fact, previous research showed that small pores between 10 and 30 nm were more efficient in trapping QDs than large pores or the outer bead surface.[17]

Doping. Single-color doping was accomplished by injecting a controlled amount of quantum dots into porous beads suspended in butanol. The mixture was vigorously vortexed or stirred until essentially no QDs were left in the supernatant solution. In one example, a 0.5 mL of 10 nM quantum dot solution in chloroform was mixed with 1 million porous beads in 10 mL of butanol, yielding a doping level of $\sim 3 \times 10^6$ dots/bead. The doping process was generally complete in less than 10 min. For multiccolor doping, different-colored quantum dots were premixed thoroughly in precisely controlled ratios. Porous beads were added to an aliquot of this premix solution. Specifically, the porous polystyrene beads were impregnated with green QDs (λ_{em} = 530 nm) and red QDs (λ_{em} = 630 nm) at 11 intensity/color combinations (including 7 single-color codes and 4 dual-color codes). After doping, the beads were isolated by centrifugation and were washed three times with ethanol.

Optical and Electron Microscopy. Doped beads were embedded in a resin called Lowicryl (Electron Microscopy Sciences, Fort Washington, PA), and were cut into 70−200-nm thin sections on an ultramicrotome machine (Leica Ultracut S, Bannockburn, IL). The thin sections were imaged on a Hitachi H-7500 transmission electron microscope (TEM) operating at 75K voltage with a magnification of 6000. True-color fluorescence images were obtained from both intact beads and thin sections by using an inverted Olympus microscope (IX-70) equipped with a digital color camera (Nikon D1), a broad-band ultraviolet (330−385 nm) light source (100-W mercury lamp), and a long-pass interference filter (DM 400, Chroma Tech, Brattleboro, VT). Wavelength-resolved spectra were obtained by using a single-stage spectrometer (Spectra Pro 150, Roper Scientific, Trenton, NJ).

Flow Cytometry. Flow cytometric analysis was performed on both FACSVantage and FACScan flow cytometers (Becton Dickinson, San Jose, CA) with a 488-nm excitation laser. Green fluorescence was detected on the FL1 channel (530/30 nm band-pass filter), and red fluorescence was collected on the FL3 channel (630/22 nm band-pass filter). Beads were analyzed at up to 5000 events/s, and data were obtained without compensation. Due to the broad excitation profiles of quantum dots, a single light source at 488 nm was used to excite both fluorescence colors.

RESULTS AND DISCUSSION

The intrinsic hydrophobic nature of polystyrene beads is well suited for incorporating TOPO-coated QDs, which move into the pores by diffusion and are trapped by strong hydrophobic interactions. We found that this partitioning process was so rapid and quantitative that essentially no dots (less than 0.1%) were left in free solution after 10 min. In addition, we observed no QD leakage when the doped beads were exposed to water or polar organic solvents such as ethanol, acetone, or acetonitrile. Figure 1 shows fluorescence images of QD-doped polystyrene beads with mesoscale 2−50-nm pores. These "monochromatic" beads were prepared by using single-color quantum dots and were mixed and spread on a glass surface for fluorescence imaging. Due to the broad excitation profiles of quantum dots, all the encoded beads were observed simultaneously with a single light source.

As shown by the enlarged images in Figure 1b, the beads are remarkably bright and uniform. Quantitative measurements using flow cytometry indicate that the porous beads are more than 1000 times brighter and 5 times more uniform in signal intensities than nonporous beads of the same size (Figure 2). Statistical analysis of the bead intensity distributions reveals a relative standard deviation of 3−4% for the porous beads and ∼15% for the nonporous beads. These values are similar to the calculated variations of the porous bead volume (3.6%) and of the nonporous bead surface area (15.3%—the outer surface area was used because there was very limited QD penetration into nonporous beads; see below). This comparison indicates that the observed signal variations are mainly determined by the intrinsic bead uniformity, not by doping statistics or measurement errors. This high level of doping uniformity achieved with porous beads allows the use of both absolute intensities and relative intensity ratios for coding. In contrast, QD-doped porous silica beads have been reported to exhibit intensity variations as large as 50% and are useful only for ratiometric coding.

We have further examined the internal structures of the mesoporous and nonporous beads by using TEM. As shown by the thin-section images in Figure 3, the porous beads have a highly porous internal structure, whereas the nonporous beads have only a small number of internal "voids" and are sealed by a ∼300-nm dense layer on the surface. This dense layer prevents QD penetration into the bead interior and limits the amount of internal space available for QD binding. In fact, high-resolution TEM

(26) Wang, Q. C.; Hosoya, K.; Svec, F.; Frechet, J. M. *Anal. Chem.* **1992**, *64*, 1232−1238.
(27) Wang, Q. C.; Svec, F., Frechet, J. M. J. *J. Polym. Sci. Polym. Chem.* **1994**, *32*, 2577−2588.
(28) Cheng, C. M.; Micale, F. J.; Vanderhoff, J. W.; El-Aasser, M. S. *J. Polym. Sci. Polym. Chem.* **1992**, *30*, 235−244.
(29) Liu, Y. L.; Svec, F.; Frechet, J. M. J.; Juneau, K. N. *Anal. Chem.* **1997** *69*, 61−65.

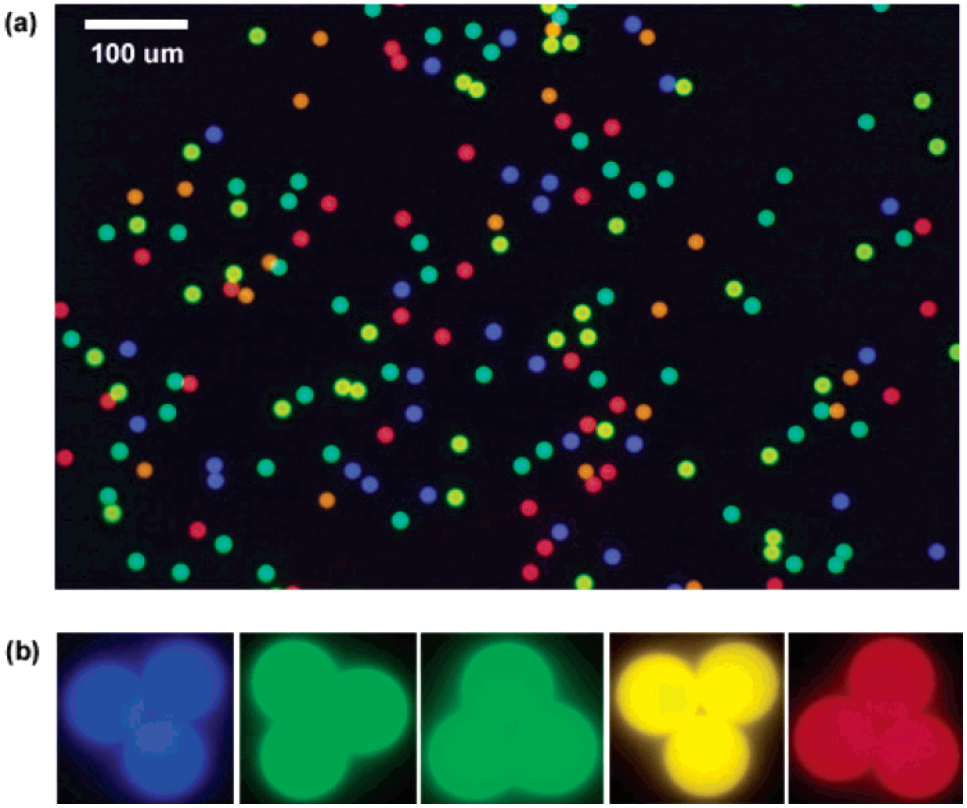

Figure 1. True-color fluorescence images of mesoporous polystyrene beads (15.4 ± 0.2 μm diameter) doped with single-color quantum dots emitting light at 488 (blue), 520 (green), 550 (yellow), 580 (orange), or 610 nm (red). (a) Wide-field view of a large population of doped beads, prepared in batches and then mixed; and (b) detailed views of monochromatic bead clusters.

imaging showed that the penetration depths of QDs into nonporous beads were limited to 10−20 nm below the surface.

Fluorescence imaging of both intact beads and thin sections shows a ring structure for nonporous beads, confirming that QDs are located on the bead surface without significant penetration (Figure 4). In contrast, fluorescence signals are highly uniform across the internal areas of the porous beads, demonstrating deep and uniform QD penetration into the bead's interior. Previous research by Frechét, El-Aasser, and co-workers[26−29] has shown that mesoporous beads have large surface areas on the order of 100−500 m^2/g, nearly 2−3 orders of magnitude larger than that of nonporous beads. Using both single-dot spectral and bulk concentration measurements,[16] we estimate that each porous bead contains as many as 20 million QDs. This level of doping corresponds to only 0.05% of the bead volume and roughly the pore surface area being occupied by QDs. The absence of fluorescence quenching or spectral shift also confirms that the embedded QDs are spatially separated and do not couple with each other. This finding is not surprising because no fluorescence resonance energy transfer was observed even at higher levels of QD doping in small beads.[16−18]

As a result of the improved signal brightness and uniformity, we have achieved high-speed readout of the encoded beads by using a standard flow cytometer. Figure 5 shows flow cytometric results obtained from a mixture of encoded beads (11 intensity/color codes plus a background control for comparison). Displayed in the form of a bivariant (two-channel) dot plot, the QD codes are detected as spatially separated clusters. Along the red fluorescence channel (*y*-axis), four intensity levels (1−4) are detected in a nearly vertical line, indicating that the red QD signal does not "spill over" into the green fluorescence channel (*x*-axis). On the other hand, the intensity levels (5−7) along the green fluorescence axis shows a positive slope, due to spectral cross-talk with the red channel. This difference can be explained by the narrow emission spectrum (full width at half-maximum, fwhm = 27 nm) of the red QDs (no overlap with the green channel) and by the broad emission spectrum (fwhm = 40 nm) of the green QDs (1−2% overlap with the red channel). For beads encoded with both green and red QDs, the coding signatures (8−11) are also detected in separate clusters, but these clusters have a distinctly elongated shape. This deviation from a circular shape arises from finite variations in the bead volume (see above discussion). As shown previously by Gao and Nie,[17] bead volume variations cause the absolute amounts of embedded green and red QDs to change simultaneously, but their relative intensity ratios remain constant for the same batch of encoded beads. The slope value for each elongated cluster is a ratiometric coding signal.[17]

Except for an error in preparing the first code (intensity too low and overlapping with the background signal), all other codes can be identified at better than 3 standard deviations (99.7 confidence level) at a readout rate as high as 1000 beads/s with an advanced flow cytometer (Figure 5 inset**)**. This readout rate is comparable to that achieved in high-speed flow cytometry using organic dyes.[30] In theory, the lifetime-limited emission rates for single quantum dots are 5−10 times lower than those of single

(30) Nolan, J. P.; Lauer, S.; Prossnitz, E. R.; Sklar, L. A. *Drug Discovery Today* **1999**, *4*, 173−180.

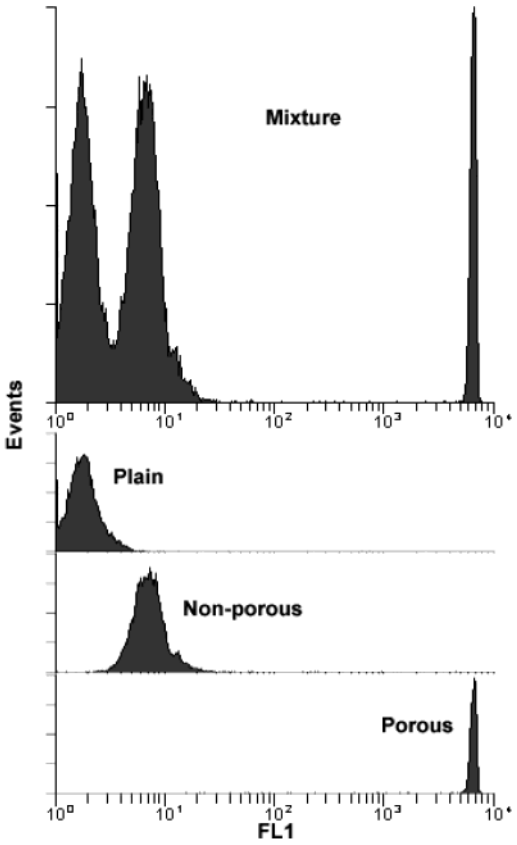

Figure 2. Quantitative flow cytometric data showing the fluorescence brightness and uniformity levels of QD-encoded porous beads, QD nonporous beads, and plain porous beads. The top histogram shows the intensity distribution of a bead mixture, and the lower three plots are separate histogram data for each type of beads. Beads were doped with green QDs and were detected on the FL1 channel (530/30 nm). A total of ~100 000 beads were analyzed at a flow rate of 5000 beads/s.

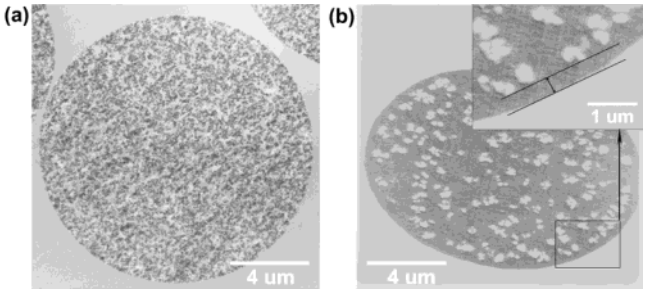

Figure 3. Transmission electron microscopy images of 200-nm thin sections obtained from (a) porous and (b) nonporous beads. A high porous internal structure was seen in the porous beads, whereas a small number of voids (bright spots) and a dense surface layer (delineated by two parallel lines) were observed in the nonporous beads.

organic dyes because QDs have excited-state lifetimes (20−30 ns) that are considerably longer than those of organic dyes (2−5 ns).[31] In practice, however, fluorescence-activated flow cytometry does not operate under lifetime-limited conditions (which would require 1−2 W of laser excitation focused to a beam size of 20 μm or less).[32] Under most experimental conditions, the rate of fluores-

(31) Dahan, M.; Laurence, T.; Schumacher, A.; Chemla, D. S.; Alivisatos, A. P.; Sauer, M.; Weiss, S. *Biophys. J.* **2000**, *78*: 2270.

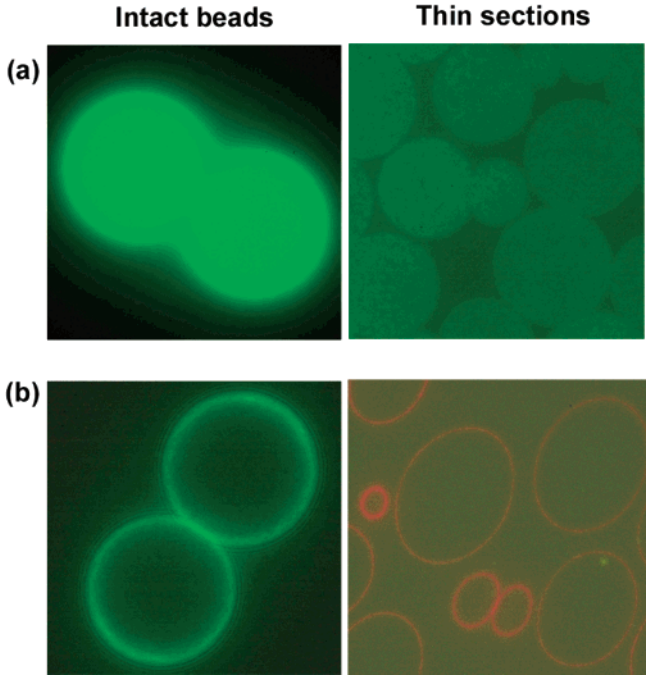

Figure 4. Comparison of quantum dot distributions inside (a) porous and (b) nonporous beads. The left-hand fluorescence images were obtained from intact beads, and the right-hand images were obtained from 200-nm thin sections. The intact porous and nonporous beads were the same size (15.4-μm diameter), but the thin sections showed various bead cross sections due to the cutting of resin-embedded beads at random axial positions. The observed elliptical shape for the nonporous beads was likely caused by an uneven or nonflat cut. Red-emitting QDs were used for visualization in the lower right image because green dots did not give enough contrast above the embedding resin autofluorescence.

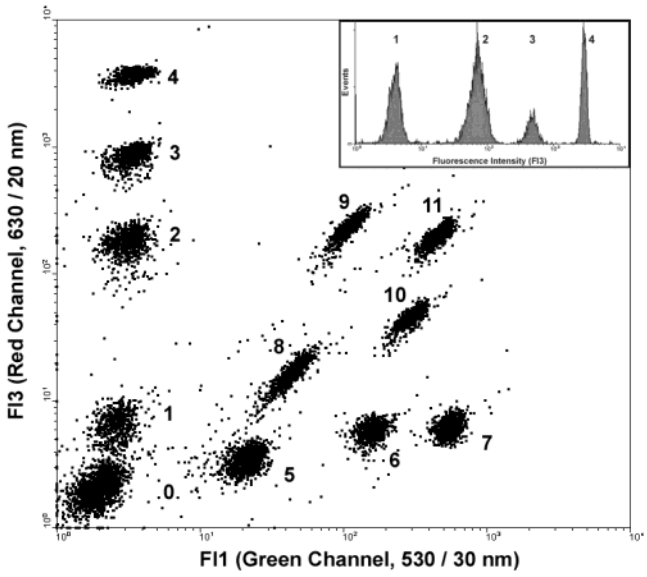

Figure 5. Two-color histogram plot showing rapid readout of QD-encoded beads with a flow cytometer. The cluster (labeled "0") at the lower left corner is for undoped control beads (background), and the other clusters correspond to QD codes 1−11. The total number of beads analyzed was ~50 000 at a speed of 500−1000 beads/s. Laser excitation wavelength 488 nm; laser power 100 mW; and size of focused laser beam 20 μm. Inset: detailed histogram plot for codes 1−4 showing the separation of peaks at three standard deviations (99.7% bead identification accuracy).

cence emission is limited by the rate of absorption. Since the molar extinction coefficients ($(0.5-2) \times 10^6\ M^{-1}\ cm^{-1}$) of QDs are about 10−50 times larger than that ($(5-10) \times 10^4\ M^{-1}\ cm^{-1}$) of organic dyes,[33] the QD absorption rate can be faster than that of organic dyes. In fact, single QDs have been found to be ∼20 brighter than organic dyes and can be imaged for an extended period of time without photobleaching.[34]

At a typical flow velocity of 3 m/s, the time for a bead to move through a 20-μm laser beam is ∼6.7 μs. During this transit time, we estimate that a single QD can emit a maximum of 100−150 fluorescence photons at 30−50% quantum yields. With an overall photon collection and detection efficiency of 1−2%, each QD would produce 1−2 photon counts when passing through the laser beam. Since 4000−5000 photon counts are likely required for accurate code identification, the minimum number of embedded QDs per bead should be at least 1000 for each color. This is a conservative estimate because using multiple spectral parameters (e.g., wavelength and lifetime), previous research has shown that the number of photons required for fluorophore identification at 99.9% accuracies is only 500.[35] This semiquantitative analysis suggests that the photon emission rates of quantum dots should be high enough for most applications in high-speed detection and imaging.

In conclusion, we have prepared a new generation of QD-encoded beads with improved coding signal brightness and uniformity. These improved features arise from the porous internal structure and the size uniformity of the mesoporous polystyrene beads prepared by porogen extraction. As a result, the QD-encoded beads have been analyzed by using a standard flow cytometer at up to 1000 beads/s. We envision that the rapid and precise procedure reported here can be extended to embed or encode a variety of porous materials with QDs and other nanospecies such as magnetic iron oxide nanoparticles and colloidal metal nanoparticles.

(32) Sondi, I.; Siiman, O.; Koester, S.; Matijevic, E. *Langmuir* **2000**, *16*, 3107−3118.

(33) Leatherdale, C. A.; Woo, W.-K.; Mikulec, F. V.; Bawendi, M. G. *J. Phys. Chem. B* **2002**, *106*, 7619−7622.

(34) Chan, W. C. W.; Nie, S. M. *Science* **1998**, *281*, 2016−2018. Chan, W. C. W.; Maxwell, D. J.; Gao, X.; Bailey, R. E.; Han, H. Y.; Nie, S. *Curr. Opin. Biotechnol.* **2002**, *13*, 40−46.

(35) Prummer, M.; Hubner, C. G.; Sick, B.; Hecht, B.; Renn, A.; Wild, U. P. *Anal. Chem.* **2000**, *72*, 443−447. Enderlein, J.; Sauer, M. J. *Phys. Chem. A* **2001**, *105*, 47−53.

ACKNOWLEDGMENT

We are grateful to Dr. Hong Yi for transmission electron microscopy and to Robert Karafa and Dr. John D. Altman for help with flow cytometry. This work was supported by grants from the National Institutes of Health (R01 GM60562) and the Coulter Translational Research Program at Georgia Tech and Emory University.

Received for review December 10, 2003. February 10, 2004.

AC0354600